

SCIENTIFIC REPORTS



OPEN

Integrated transcriptome and *in vitro* analysis revealed anti-proliferative effect of citral in human stomach cancer through apoptosis

Sri Renukadevi Balusamy¹, Sivasubramanian Ramani¹, Sathishkumar Natarajan², Yeon Ju Kim³ & Haribalan Perumalsamy³

Cancer is the second leading cause of death globally, particularly stomach cancer is third most common causes of cancer death worldwide. Citral possesses anti-tumor activity in various cancer cell lines, However its effect toward stomach cancer and its mechanism of action is have yet to be elucidated. The goal of the present study is to elucidate the role of citral in stomach cancer using transcriptome and *in vitro* approaches. We performed transcriptome analysis using RNA-seq and explored its capability to persuade apoptosis in AGS human stomach cancer cell lines *in vitro*. Furthermore, the enrichment and KEGG pathway results suggested that there are several genes involved to induce apoptosis pathway. Furthermore, our study also demonstrated that citral arrested colony formation and migration of cancer cells significantly than that of untreated cells. RNA-seq revealed a total of 125 million trimmed reads obtained from both control and citral treated groups respectively. A total number of 612 differentially expressed genes (DEGs) were identified which includes 216 genes up-regulated and 396 genes down-regulated genes after treatment. The enrichment analysis identified DEGs genes from transcriptome libraries including cell death, cell cycle, apoptosis and cell growth. The present study showed the significant inhibition effect upon citral by regulating various genes involved in signaling pathways, inhibits metastasis, colony formation and induced apoptosis both *in silico* and *in vitro*.

Stomach cancer is the third most among common cancer and second leading cause of death in the world^{1,2}. The gastric cancer is often detected in an advanced stage and therefore the treatment was not highly successful and led to median overall survival³. A recent study was conducted to explore the epigenetic inhibitors of gastric cancer cell proliferation. Epigenetic modifications play a key role in gastric cancer proliferation which has been shown to link between development and progression of gastric cancer. When screening the library of epigenetic inhibitors, BET family of bromodomain was identified to show significant inhibitory effect of gastric cancer cells and could play a significant role in gastric cancer inhibition and clinical trials has also started recently. However, it has shown some resistant mechanisms in gastric cancer cells⁴⁻⁷. Chemopreventive technique is a promising approach which implies specific natural and chemical targets to suppress, prevent or reverse the precancerous cells from progressing into invasive cancer. There are certain dietary agents especially medicinal plants and phytoconstituents has been receiving interest as the possible chemopreventive agents over the past decades⁸.

Previous studies demonstrated the modulation of dietary habits with high intake of fruits, and vegetables rich in antioxidants can minimize the gastric cancer rate. The patients with gastric cancer are highly influenced by reactive oxygen species dependent lipid peroxidation that resulted due to insufficient antioxidants⁹. Specifically,

¹Department of Food Science and Biotechnology Sejong University, Gwangjin-gu, Seoul, Republic of Korea.

²Department of Horticulture, Suncheon National University, Suncheon, Republic of Korea. ³Graduate School of Biotechnology, College of Life Science, Kyung Hee University, Yongin, 446- 701, Republic of Korea. Sri Renukadevi Balusamy and Haribalan Perumalsamy contributed equally. Correspondence and requests for materials should be addressed to S.R.B. (email: srirenukadevibalusamy@gmail.com) or Y.J.K. (email: yeonjukim@khu.ac.kr) or H.P. (email: harijai2004@gmail.com)

fruits rich in vitamin c prevent the development of gastric cancer by delaying tumor progression in experimental animals¹⁰. These delaying actions may be due to any one of the combinational mechanisms: procarcinogen activation prevention, inactivating carcinogens, stimulating DNA repair mechanisms, down-regulating protooncogene expression, up-regulation of tumor suppressor genes, inhibition of cell proliferation, differentiation induction and promoting apoptosis, stimulation of immune system, and regulating transcription factors and abnormal signaling pathways^{11,12}. Therefore, identifying the targets that can inhibit the growth of tumor cell by inducing apoptosis is one of the best strategies.

Cymbopogon citratus (D.C.) Stapf. commonly known as lemon grass oil distributed in all tropical and subtropical countries. Lemon grass is used for making soft drinks and as an aroma for making herbal tea. The aerial parts of lemon grass are also widely used in folk medicine to treat various diseases including digestive disorders, inflammation, diabetes, nervous disorders, and several other health problems¹³. It is also reported to possess antioxidants that scavenge free radicals and can be used in the prevention of several life-threatening diseases such as atherosclerosis, heart diseases, cancer and arthritis in which reactive oxygen species (ROS) play a crucial role. ROS generation is also associated with diseases in gastrointestinal tract^{13,14}. Next generation sequencing (NGS) made feasible to analyze large-scale screening transcriptome that discovered genes at genome level without the reference genome sequences. Transcriptome analysis along with bioinformatic data mining tools provides the platform to simultaneously interpret various genes, identify the targets and its interactions after treatments. There are several previous studies demonstrated the role of citral on inhibiting the growth of cancer cells by targeting molecular signaling pathways including small-cell lung cancer; breast cancer-MDA-MB-231; Colorectal cancer^{15,16}. This is the first report to combine both RNA seq and *in vitro* analysis to prove the effect of citral on suppressing stomach cancer growth by promoting apoptosis.

Results and Discussion

Isolation of citral from *Cymbopogon citratus* oil. The major active constituent citral was isolated identified through various spectroscopic analyses; including electron ionized mass spectrometry (EI-MS) and nuclear magnetic resonance (NMR) spectroscopy. Citral was identified based on the following evidence: a colorless oil; UV (methanol): λ_{\max} nm = 233; EI-MS (70 eV), *m/z* (% relative intensity): 152 [M]⁺ (6.4), 137 (3.8), 94 (12.5), 84 (24.6), 69 (100), 59 (3.40), 41 (87.3), ¹H NMR (DMSO, 600 MHz): δ 1.62 (3 H, s), 1.67 (3 H, d, *J* = 1.2 Hz), 2.00 (2 H, s), 2.18 (3 H, m), 2.62 (2 H, t), 5.20 (1 H, m), 5.83 (1 H, t), 9.96 (1 H, d, *J* = 8.16 Hz). ¹³C NMR (CDCl₃, 150 MHz): δ 192.4 d (C-1), 166.1 s (C-3), 134.4 s (C-7), 128.4 d (C-2), 123.5 d (C-6), 40.4 t (C-4), 26.9 t (C-5), 25.1 q (C-8), 18.1 q (C-9), 17.8 q (C-10) (Supplementary Fig. S1).

Citral inhibited cancer viability by altering cell morphology. The inhibition of cell proliferation occurred after treatment with citral (Fig. 1A) at various concentrations (7.5, 12.5, 25, 50, 100, 200 μ g/mL) in AGS cell lines. The photographs and calculation of IC₅₀ were performed after 48 h of treatment (Fig. 1B–D). The 5 μ g/mL of citral treated cells showed gradual change in the morphology and extended its determined alteration at 40 μ g/mL respectively. All the treated samples tend to show distinct phenotype including shrunken cells, shapeless and significantly reduce in cell number. Whereas, non-treated cells showed no difference in morphology and displayed 90% confluent cells. Various plant essential oils decrease the various cancer cell growth by inducing decrease in cell number, cell morphology and cytoplasmic vacuolation and nuclei^{17,18}.

RNA sequencing analysis. To identify the expression pattern of apoptosis related genes after citral treatment in AGS cell line RNA sequencing were performed. At first, isolated RNA quality and concentration was measured by using Agilent 2100 BioAnalyzer. The high-quality samples were considered to perform paired end (PE) RNA sequencing with control (non-treated) and citral treated samples using the Illumina Hiseq 2500 platform. Supplementary Fig. 2 represents quality of RNA isolation and Phred score results of the control and citral (20 μ g/mL) in AGS. After sequencing, the quality of reads of each sample were evaluated using FastQC (version 1.0.0) based on Phred quality score (ref: <https://www.ncbi.nlm.nih.gov/pubmed/9521921>). A total of 140 million paired end reads with average of 70 million reads per sample were generated from RNA sequencing and their summary of transcriptome statistics were described in Table 1. Furthermore, low quality reads and adaptor sequences were removed with high stringency filtering yielded that 125 million reads (average of 63 million per accession). In total, 85.57% and 80.49% reads was mapped (average of 83%) on the reference h19 genome to the control and citral treated respectively. The raw reads in FASTQ format which supporting this study obtained from paired-end (PE) RNASeq libraries have been deposited into Sequence Read Archive (SRA) database under National Center for Biotechnology Information (NCBI) accession number SRP150561 (<https://www.ncbi.nlm.nih.gov/sra/SRP150561>).

Differential expression analysis. The cufflinks program was used to normalize and measure relative abundance of reads through fragments per kilobase million (FPKM) and density expression levels of control and citral treated libraries based on log₁₀ value of FPKM were represented in Supplementary Fig. 3. Then, while comparing normal with citral treated AGS cells, a total of 612 differentially expressed genes (DEGs) were identified based on statistical significance values of fold change ≥ 2 and *p*-value < 0.05 . Among all those genes, 216 and 396 genes were up-regulated and down-regulated respectively. The significantly expressed genes were shown as Supplementary Fig. 3 and entire list of identifying differently expressed genes were given as Supplementary File S6.

Enrichment analysis. The identified DEGs were investigated into functional enrichment analysis. Network of DEG and network between up-regulated DEG and relative external genes is shown (Figs 2 and 3; Supplementary Files 1 and 2) based on gene enrichment. The GO terms mainly include three major categories of biological process (BP), molecular function (MF) and cellular component (CC). The gene ontology of 216 DEG

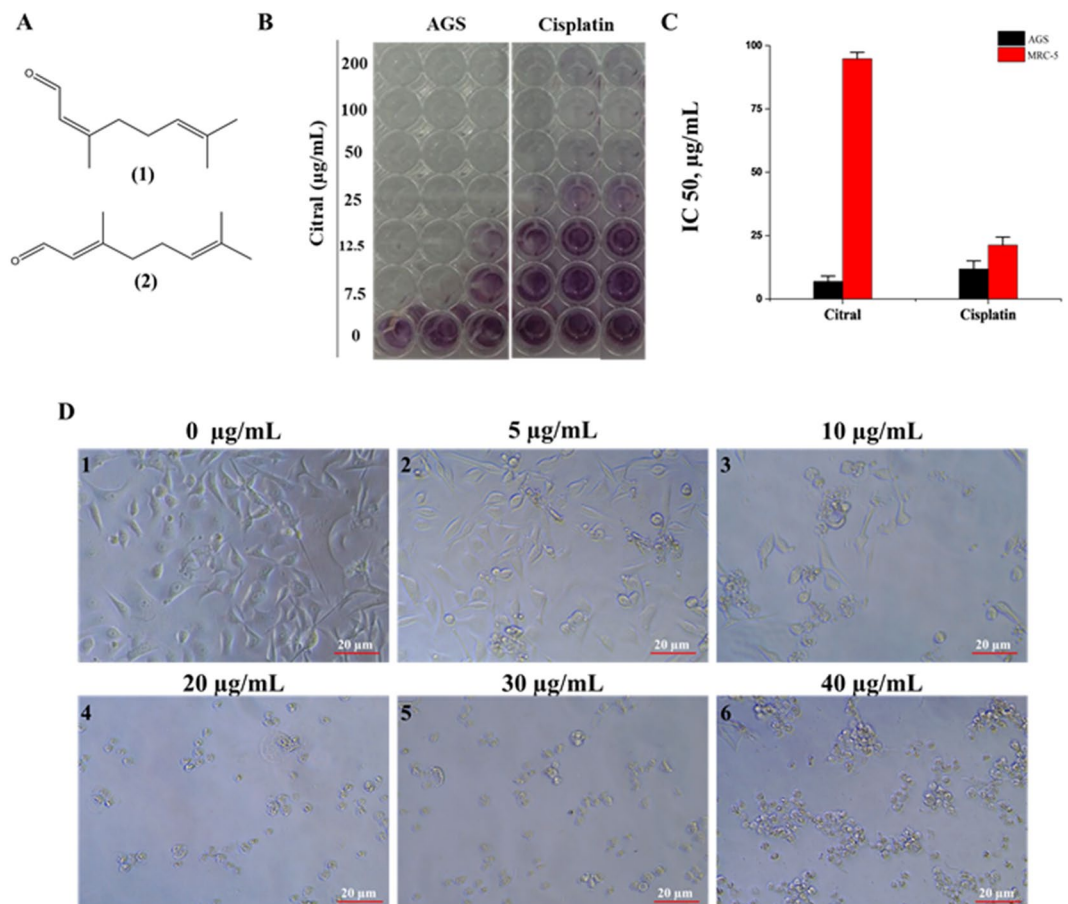


Figure 1. Decreased cell viability and morphological changes after citral treatment. (A) The chemical structure of cis- (neral) and trans-citral (geranial). (B) The image was captured right after performing MTT assay. (C) Inhibitory concentration (IC₅₀) of citral towards AGS cancer cells was compared with positive control cisplatin. X-axis indicate compounds treated for cell lines and Y-axis indicate IC₅₀. Cell toxicity of citral was compared with normal cell line MRC-5. (D) Morphological characteristics of AGS cell lines were observed after the treatment.

Library	Total reads	Reads length (bp)	Trimmed reads	Mapped reads	Mapping reads (%)
Control	75,171,336	101	74,990,756	64,170,781	85.57
Treated	65,905,230	101	51,385,566	41,357,663	80.49

Table 1. The statistics summary of RNA-Seq libraries.

resulted in 196 recognized genes thus further analysis is proceeded with these 196 genes with GO terms (Fig. 4). The detail information is given in the Supplementary Files 3–5. The enrichment results are projected here for BP (Fig. 5), MF (Fig. 6) and CC (Fig. 7) respectively. Further analysis of GO subcategories, observed that *PCK2*, *IFI6*, *LGALS3BP* and *EDAR* genes were mainly involved in down-regulation upon citral treatment while *PLCG2*, *ZFAND2* and *HSPB1* DEGs genes were up-regulated (Supplementary File S6). Furthermore, KEGG pathway analysis revealed that significantly enriched DEGs were grouped into 46 known pathways (Supplementary File S7).

Enrichment analysis of DEGs with associated apoptosis. Cell death specifically apoptosis is one of the most vital studied candidates among cell biologists. Therefore, detail study of pathways involved in cell death is essential to gain insights into pathogenicity of the disease and can pave the way to identify the possibilities of treating the disease. KEGG analysis revealed that MAPK signaling pathway, NF-kappa B signaling pathway, p53 signaling pathway, PI3-K-Akt signaling pathway, pathways in cancer, and prostate cancer pathways are mostly enriched in up and down-regulated genes which identified between normal and citral treated samples in AGS. Among them, cell cycle, pathways in cancer, and MAPK signaling pathways were observed as mostly enriched pathways. In addition, several common genes were identified in these pathways were listed in Table 2. Among them, cell cycle (hsa04110) and cancer (hsa05200) occupied several down-regulated DEG genes. The genes involved in cell cycle synthesis are very crucial for the inhibition of cancer cell progression¹⁹. For example,

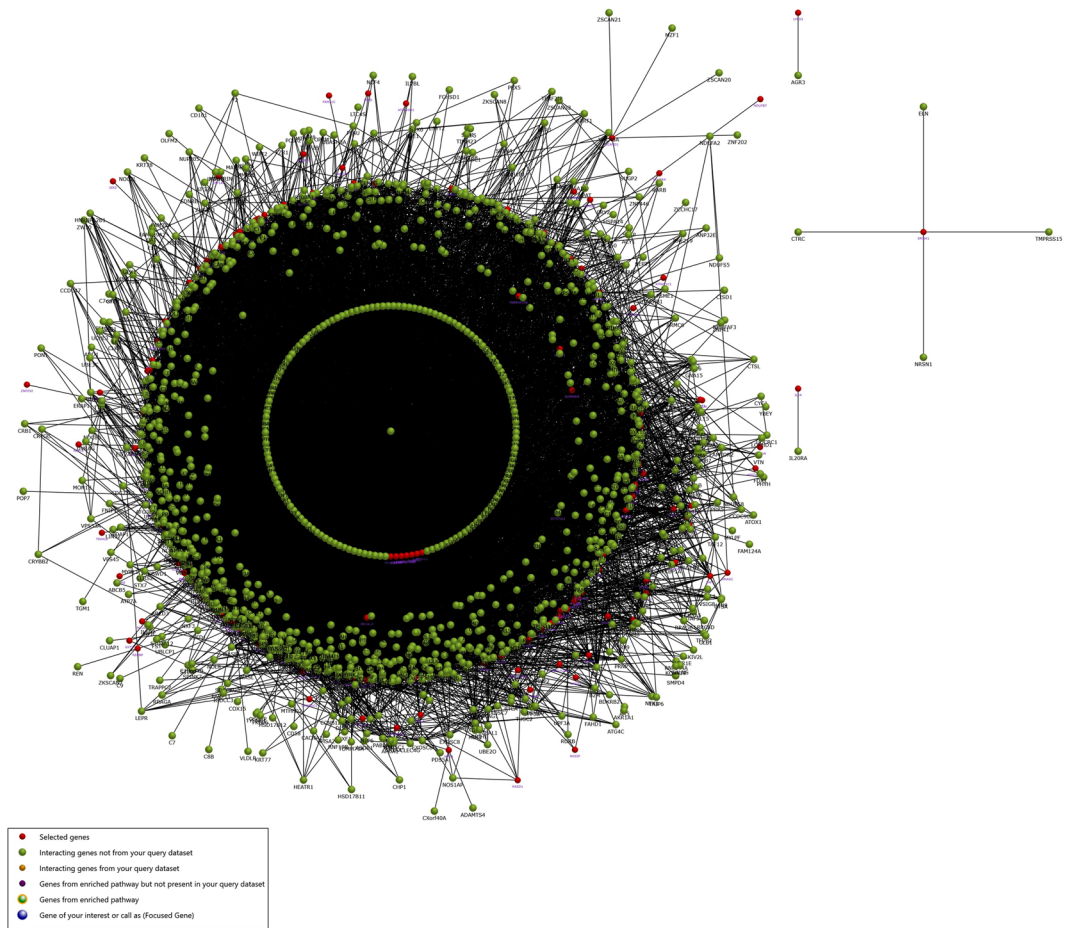


Figure 2. Functional enrichment based interaction of up-regulated DEGs with related external genes.

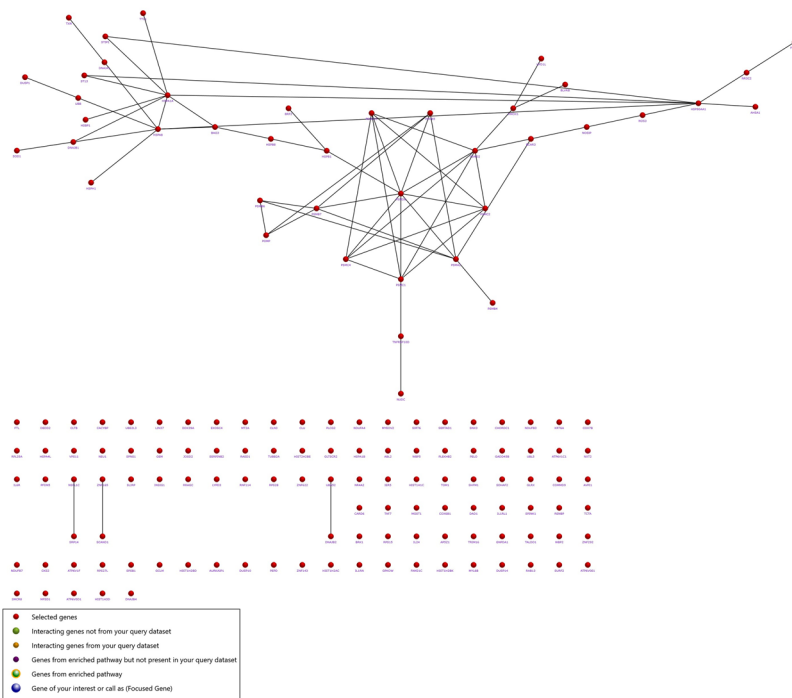


Figure 3. Functional enrichment based interaction network of DEGs of citral treatment groups.

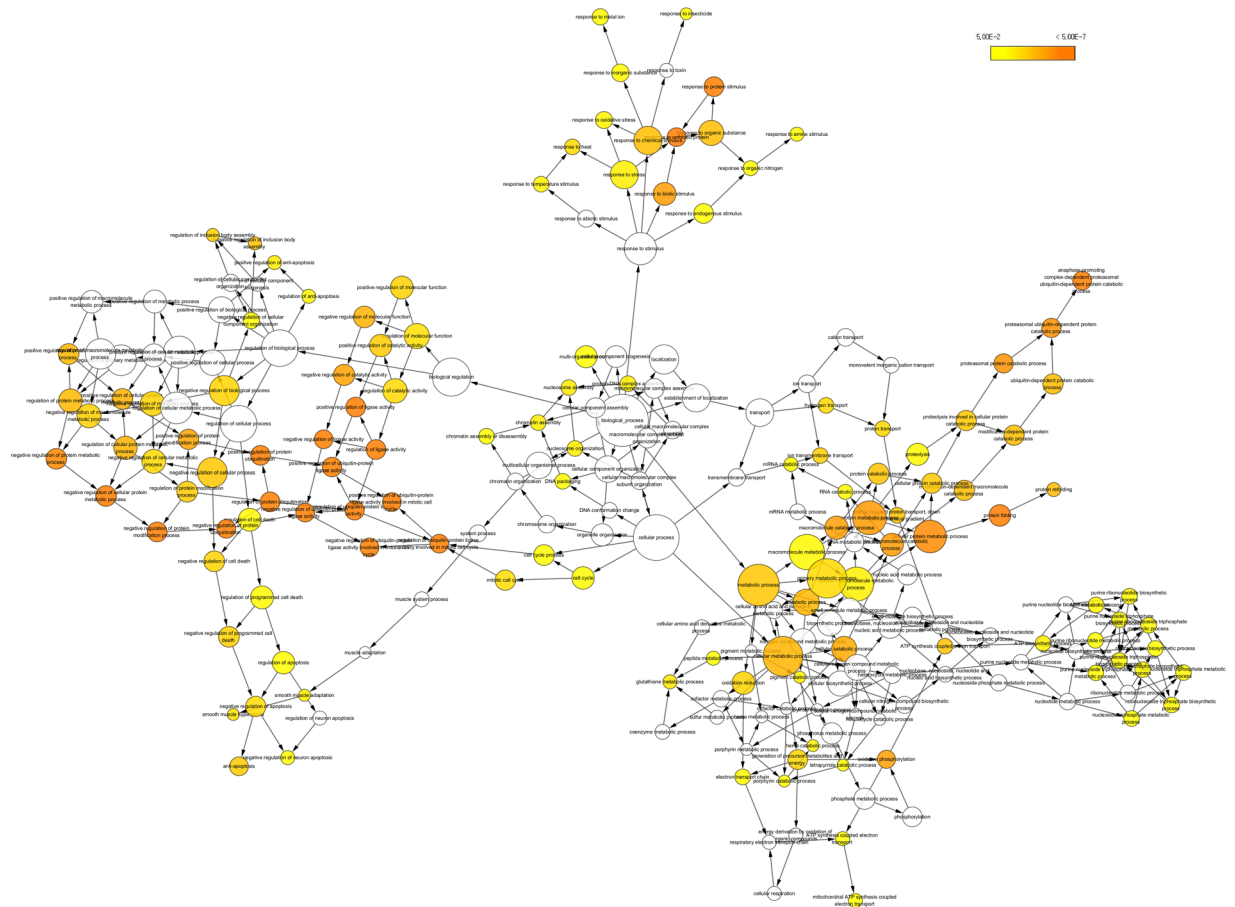


Figure 4. Network visualization of significantly overrepresented GO terms.

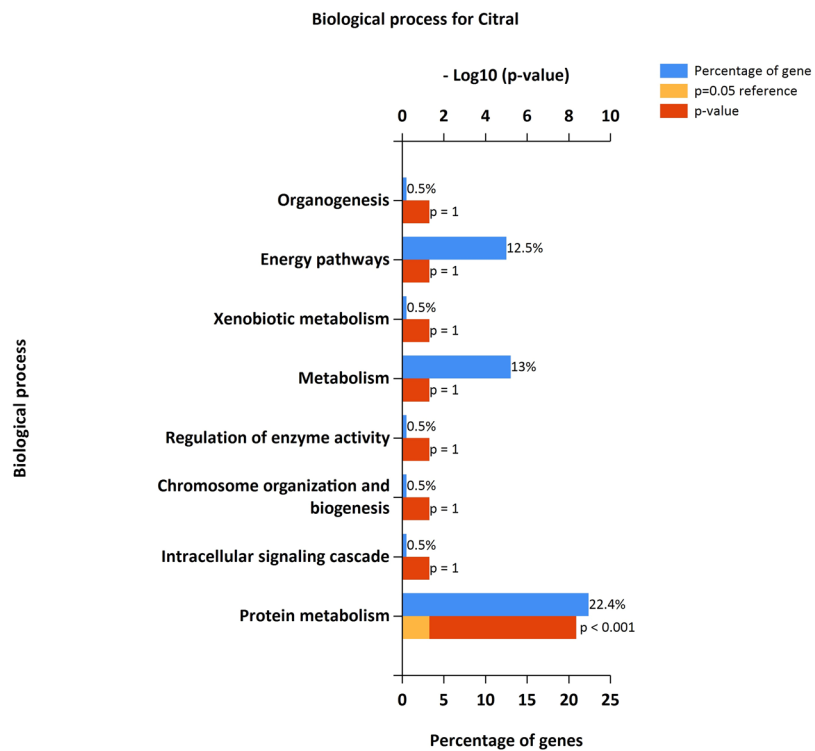


Figure 5. Functional gene enrichment analysis of identified DEG as biological process.

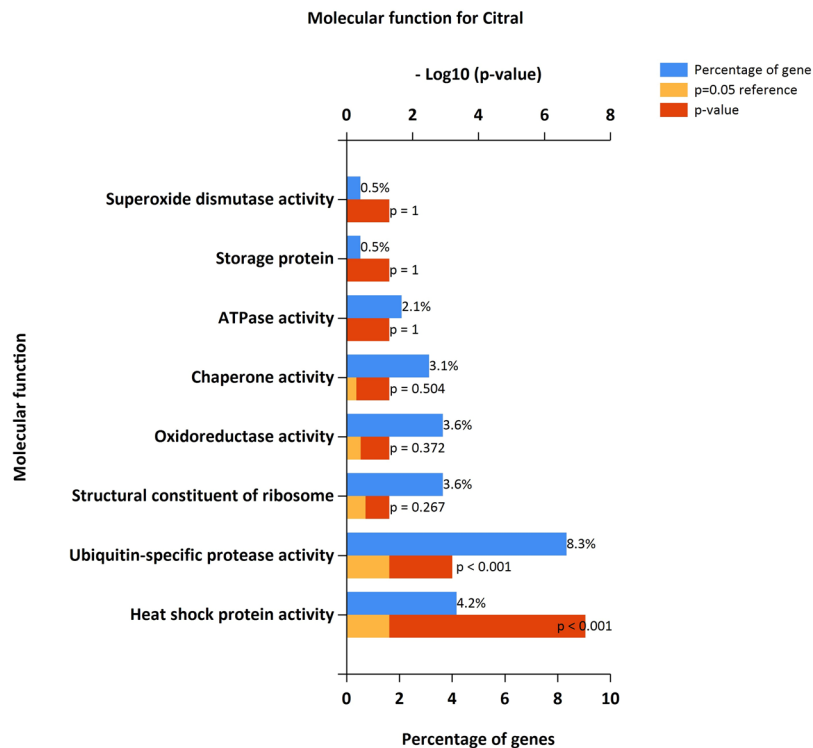


Figure 6. Functional gene enrichment of DEG as molecular function.

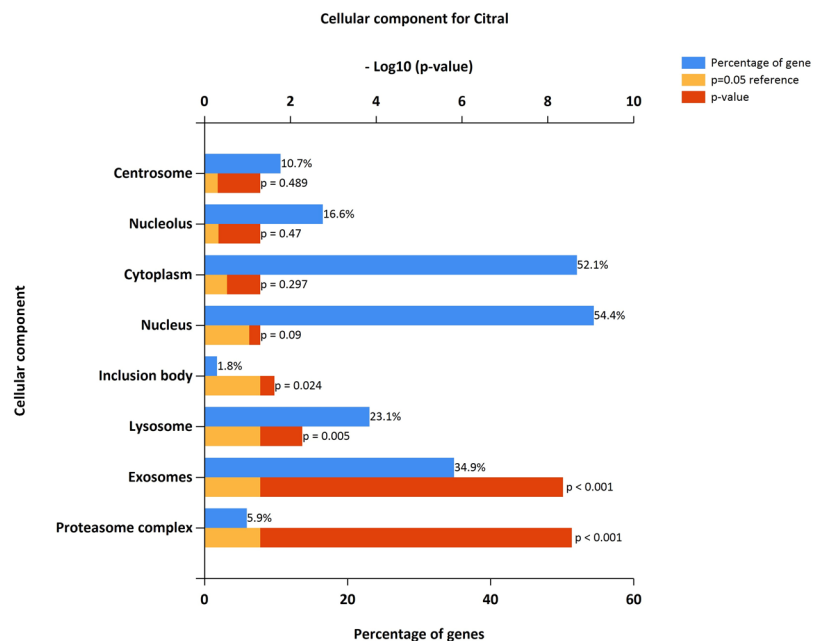


Figure 7. Functional gene enrichment of DEG as cellular component.

cyclin-dependent kinases (CKD2) are the most important regulators for the transition and cell cycle progression and play a significant role in regulating cell cycle division including centromere duplication, DNA synthesis, G1-S transition, and modulation of G2 progression^{20–22}. Furthermore, the enrichment analysis and KEGG pathway results indicated that, there are several genes involved to initiate apoptosis pathway that are directly/indirectly related to the treatment of citral. In addition, enrichment analysis identified DEGs genes from transcriptome libraries were mainly involved in cell death, cell cycle, apoptotic process, and cell growth (Table 3).

Differential expressed genes	KEGG	Pathway	Genes involved	Log2(fold change)
Up-regulated genes	hsa04101	MAPK signaling pathway	HSPA1A, HSPA1B, GADDA45B	8.09
	hsa04064	NF-kappa B signaling pathway	PLCG2	5.42
	hsa05200	Pathways in cancer	PLCG2, HSP90AA1, CKS2	5.42
	hsa05215	Prostate cancer	HSP90AA1	3.57
	hsa04151	PI3K-Akt signaling pathway	HSP90AA1, ILR6	2.54
	hsa04115	p53 signaling pathway	GADD45B	2.54
	hsa04210	Apoptosis	TNFRSF10D	1.85
	hsa03040	Spliceosome	SYF2	1.67
Down-regulated genes	hsa05200	Pathways in cancer	MSH6, MSH2, COL4A5, MMP1, CDK2, CCNE2, LAMB1, RAD51, PDGFRA	-1.17
	hsa04110	Cell cycle	CCNE1, CCNB3, CHEK1, CCNB1, CDK2, CDC7, E2F1, WEE1, CCNA2, MCM3, TTK, MCM6, CDC6, PKMYT1, BUB1B, PLK1, ESPL1	-1.25
	hsa05222	Small cell lung cancer	CCNE1, LAMB1, E2F1	-1.25
	hsa04151	PI3K-Akt signaling pathway	CCNE1, COL4A5, COL27A1, LAMB1, PDGFRA, PCK2	-1.25
	hsa04115	p53 signaling pathway	CCNB3, CCNB1, CDK2, CCNE2, RRM2, SERPINE1	-1.27
	hsa05210	Colorectal cancer	MSH2	-1.65
	hsa05202	Transcriptional mis-regulation in cancer	WHSC1, NUPR1	-1.68
	hsa04010	MAPK signaling pathway	CACNG8, MAP3K5, DUSP6, RPS6KA2, RPS6KA5, PDGFRA	-1.76
	hsa05219	Bladder cancer	MMP1, VEGFA, E2F1	-1.80
	hsa03320	PPAR signaling pathway	MMP1, SLC27A2, PCK2	-1.80
	hsa01212	Fatty acid metabolism	HADH, E2F2	-1.93
	hsa05205	Proteoglycans in cancer	VEGFA, VTN	-1.97
	hsa04064	NF-kappa B signaling pathway	TRAF5	-2.15
	hsa05215	Prostate cancer	E2F1	-2.24
	hsa04152	AMPK signaling pathway	CCNA2, CFTR, PCK2	-2.26
	Hsa05223	Non-small cell lung cancer	E2F2	-4.03

Table 2. KEGG enrichment analysis of identified DEG genes from control and citral treated samples in AGS.

Regulation of apoptosis related genes under citral treatment. RNA-seq data after citral treatment resulted in involvement of both up- and down- regulation of apoptosis pathway related genes. There are several genes up-regulated upon citral treatment and are involved in biological function (Table 4). Our results were also in agreement with several previous studies in various cancer types. For instance, IL-24 function is to induce cancer cell apoptosis through the down-regulation of Bcl-2 expression which is a key factor involved in mitochondrial mediated apoptosis²³. Similarly, the intron region of p53 directly binds to the ribosomal protein RPS27L and induced apoptosis in various cancer models both *in vitro* and *in vivo*²⁴. Apoptosis mechanism is a normal programmed death process which is very crucial for maintaining disease free body. Several genes that are associated with negative regulation of apoptosis can inhibit the apoptosis process and thus result in the cancer cell progression. Our result suggests that upon citral treatment, several genes involved in negative regulation of apoptosis pathways including *IF16*, *DHRS2*, *IFIT3*, *CEACAM5*, *PLK*, *ICDK1* and so on. (Table 5) are down-regulated upon citral treatment. Apart from this, there is down-regulation of genes involved in positive regulation; indicating that these genes have less significant role in inducing apoptosis after citral treatment.

Citral reduced stomach cancer cell proliferation by inhibiting colony formation. Colony formation assay is performed to identify the citral ability to inhibit the growth of AGS cells as well as to indirectly monitor the cell death²⁵. For the treatment of the cell lines, different concentration of citral from 5, 10, 25, 50, 100 µg/mL were used respectively. The experiment was carried out for continuously for 7 days in a 6-well plate by changing fresh media and every 2–3 days. The non- treated cells showed colony formation and amplified the cell number with increased colony formation (Fig. 8A,B). Whereas, the treated cells even at 5 µg/mL showed decreased in colony number and induced the cell death thus specifying that citral has a role to be used as anti-proliferative drug. The total number of colonies were calculated using cell counter (imageJ software) and it was plotted (Fig. 8C).

Migration ability of cancer cell was inhibited by citral treatment. We have assessed the invasion and metastatic stage of AGS cell line after citral treatment. The growth effect and migration was affected in cancer cell by the treatment of citral in various concentration (0, 5, 10, 20, 30, 40 µg/mL) (Fig. 8D2–D5). In case of control, cancer cells exposed completely grown migrated cells (Fig. 8D1). The cancer cell progression is the sequence of occurrences essential to the development of metastasis and cell invasion. Once the cells can invade the nearby tissues, these cells pass through the base membrane and extracellular matrix and further penetrate to the lymphatic and vascular circulation. Ultimately, cells grow in the new area and proliferate to produce secondary tumor²⁶. However, citral treatment inhibited the cell invasion and migration of AGS cells and thus prevented these consequences.

DEG							
Go terms	Category	Number of genes	Go id	p-value	Up-regulated genes	p-value	Down-regulated genes
Response to unfolded protein	BP	8	GO:006986	1.79E-09	HSPA4L, DNAJA1, HSPA8, HSPH1, HSP90AA1, DNAJB1, DNAJB4, HSPB1	NA	NA
Negative regulation of programmed cell death	BP	2	GO:0043069	0.62	PLCG2	0.33	KANK2
Negative regulation of cell death	BP	4	GO:0060548	0.77	HSPA1A, CACYBP, HSPA1B	0.57	SRGAP2
Regulation of cell cycle	BP	19	GO:0051726	1.64E-05	GADD45B, HSPA8	1.64E-05	E2F2, RBL1, MYBL2, PLK1, PLK1, GTSE1, WEE1, MX2, PKMYT1, CCNE, CDC25A, CCNB2, PKD2, MASTL, SRC, NUPR1, RPS6KA2
Negative regulation of programmed cell death	BP	2	GO:0043069	0.62	PLCG2	0.33	KANK2
Positive regulation of cell death	BP	1	GO:0010942	0.12	PRODH	NA	NA
Negative regulation of cell death	BP	4	GO:0060548	0.77	HSPA1A, CACYBP, HSPA1B	0.57	SRGAP2
Intracellular membrane-bounded organelle	CC	10	GO:0043231	NA	NA	0.67	MCM3, CHAF1A, SAMD9, OAS2, SLC7A5, DBF4B, DNMT3B, LIG1, BARD1, ATP8A1
Negative regulation of cell growth	BP	2	GO:0030308	NA	NA	0.87	APBB2, CAPRIN2
Negative regulation of catalytic activity	BP	1	GO:0043086	0.64	CLN3	NA	NA
Cell cycle arrest	BP	4	GO:0007050	NA	NA	0.64	APBB2, PKD2, PKD1, BARD1
Negative regulation of growth	BP	2	GO:0045926	0.40	MT1X, MT2A	NA	NA
Cellular protein metabolic process	BP	5	GO:0044267	NA	NA	0.64	IGFBP4, HSPG2, IGFBP2, UBE2L6, LYZ
Positive regulation of cellular protein metabolic process	BP	1	GO:0032270	NA	NA	0.76	UHRF1

Table 3. Functional enrichment analysis of DEGs genes involved in apoptosis pathway after citral treatment. BP: Biological process; CC: Cellular component; NA Not available.

Citral induced apoptotic effect in human stomach cancer cell lines *in vitro*. The human body generates 10–100 billion cells every day and the equal number of cells dies to maintain homeostasis. Under this condition, cell death occurs mainly by undergoing apoptosis which is silent process²⁷. However, cancer cells modulate the apoptosis process by transcriptionally, translationally and even by post-translational modification and thus resulting in cancer cells to escape apoptotic process²⁸. Therefore, identifying the target that increase the apoptosis in cancer cells is one of the best strategies^{29,30}. Our RNA-seq data also demonstrated there is occurrence of apoptosis after citral treatment (Supplementary File S6). In order to confirm it *in vitro*; we performed various assays that can confirm the apoptosis. The hoechst staining was performed to study the condensation and apoptosis happened after treatment of citral to cancer cells. Our results demonstrated that upon citral treatment, there is visible chromatin condensation and degradation of nuclei of AGS cells happened at different concentration of citral treatment. In untreated state, the cell membrane present in its undamaged form and the dye is unable to diffuse into the nuclei and has no fluorescence (Fig. 9A1). However in 5 µg/mL of citral treatment, cells started to show chromatin condensation and fragmented/shrunken nuclei like structures due to damage of cell membrane. The intensity of damage increase when the concentration of citral increases (Fig. 9A2–A6). When looking inside the cell, one of the most obvious features of apoptosis is condensation of the nucleus and its fragmented segments³¹. Annexin-V-FITC results also exhibited that citral inhibited together early and late apoptosis in AGS cells. In the concentration of 10 µg/mL citral showed maximum accumulation of late apoptosis (Q2) and moderate number of cells undergone early apoptosis (Q4) (Fig. 9B2). Whereas, 20 µg/mL of citral treated cells exhibited maximum number of early apoptotic cells (Q2) and moderate amount of late apoptosis respectively (Q4) (Fig. 9B3). Later, the propidium iodide (PI) staining was performed to determine the dead cells and live cells. This dye is particularly permeable in the dead cells because the dye can easily penetrate the damaged cell and thus resulted in the bright fluorescence. The cells treated with citral (10 and 20 µg/mL) showed bright fluorescence with decrease in cell number and reduced cell viability (Fig. 9C2–3). In contrast, the cells stained without treatment showed the absence of fluorescence clearly indicating that cells are intact (Fig. 9C1). Finally, the DNA fragmentation after citral treatment was assessed. The untreated cells showed the presence of intact DNA however, the cells treated with different concentration (5, 10 and 20 µg/mL) showed there is gradual increase in degradation of DNA occurred (Fig. 9D). The breakdown of DNA into small fragments is one of the characteristic features of apoptosis^{31,32}.

Materials and Methods

Reagents, chemicals and cell lines. Commercially available anticancer drug cisplatin, and MTT (Thiazolyl blue tetrazolium bromide) were obtained from Sigma-Aldrich (St. Louis, MO). The culture medium, serum and phosphate buffer were purchased from by Life Technologies (Grand Island, NY). Antibiotic-antimycotic solution and 0.5% trypsin-ethylenediaminetetraacetic acid (EDTA) was obtained from Invitrogen (Grand Island, NY, USA). Citral essential oil was acquired from Berjé (Carteret, NJ, USA). All the other chemicals and reagents used in this study were of reagent-grade quality and available commercially. The cancer cell lines (AGS: ATCC-CRL-1739), Human lung normal cell lines (MRC-5: ATCC-CCL-171) were cultured in RPMI 1640

Go terms	Go ids	Category	p-value	Genes
BP	GO:0006915	Apoptotic process	0.54	IL24
BP	GO:0043066	Negative regulation of apoptotic process	0.46	CLN3
BP	GO:0043066	Negative regulation of apoptotic process	0.46	UBA52
BP	GO:0043065	Positive regulation of apoptotic process	0.52	UBA52
MF	GO:0008656	Cysteine-type endopeptidase activator activity involved in apoptotic process	0.36	RPS27L
BP	GO:0006919	Activation of cysteine-type endopeptidase activity involved in apoptotic process	0.73	RPS27L
BP	GO:0043065	Positive regulation of apoptotic process	0.52	SOD1
BP	GO:0043066	Negative regulation of apoptotic process	0.46	SERPINB2
BP	GO:0043065	Positive regulation of apoptotic process	0.52	HMOX1
BP	GO:0043066	Negative regulation of apoptotic process	0.46	UBB
BP	GO:0043065	Positive regulation of apoptotic process	0.52	UBB
BP	GO:0043065	Positive regulation of apoptotic process	0.52	GADD45B
BP	GO:0006915	Apoptotic process	0.54	GADD45B
BP	GO:0043066	Negative regulation of apoptotic process	0.46	DNAJA1
BP	GO:0043065	Positive regulation of apoptotic process	0.52	DNAJA1
BP	GO:0043065	Positive regulation of apoptotic process	0.52	CLU
BP	GO:0042981	Regulation of apoptotic process	0.59	DEDD2
BP	GO:0043065	Positive regulation of apoptotic process	0.52	OSGIN1
BP	GO:0010664	Negative regulation of striated muscle cell apoptotic process	0.26	BAG3
BP	GO:0043066	Negative regulation of apoptotic process	0.46	BAG3
BP	GO:0043066	Negative regulation of apoptotic process	0.46	HSPB1

Table 4. The identified up-regulated genes list after citral treatment in AGS cell lines. BP: Biological process; MF: Molecular function.

containing 10% FBS and 1% antibiotic-antimycotic solution under 5% CO₂ and 95% air at 37 °C, whereas MRC-5 cell lines were cultured with DMEM containing 10% FBS, 1% antibiotic-antimycotic solution and 1% glutamine.

Medium pressure liquid chromatography (MPLC). The lemongrass oil (5 g) was monitored by TLC on silica gel plates (Silica gel 60 F₂₅₄) developed with hexane and ethyl acetate solvent system. Based on TLC pattern result it was separated by MPLC using a Biotage Isolera apparatus equipped with a UV detector at 254 nm and 365 nm and a column cartridge SNAP (100 g silica gel) with column volume 132 mL. Separation was achieved with a gradient of hexane and ethyl acetate [100:0 (264 mL), 9:1 (396 mL), 8:2 (396 mL), 7:3 (660 mL), 6:4 (264 mL), 5:5 (264 mL), 3:7 (264 mL), and 1:9 (132 mL) by volume] at a flow rate 25 mL/min to provide 105 fractions (each about 22 mL). Column fractions were monitored by TLC on silica gel plates (Silica gel 60 F₂₅₄) developed with hexane and ethyl acetate (8:2 by volume) mobile phase. Fractions with similar *R_f* values on the TLC plates were pooled. Spots were detected by spraying with 5% sulfuric acid and then heating on a hot plates stated previously. A preparative high-performance liquid chromatography (HPLC) was performed to separate the constituents from active fractions. The column was a 7.8 mm i.d. × 300 mm μBondapak C18 (Waters, Milford, MA, USA) with a mobile phase of methanol and water (85:15 by volume) at a flow rate of 1 mL min⁻¹. Chromatographic separation was monitored using a UV detector at 233 nm. Finally, an active constituent 1 (citral) (28 mg) was isolated at a retention time of 13.8 min.

Cell viability assay. The anti-proliferative activity of citral toward AGS was evaluated using an MTT assay. The MTT assay was performed as those stated previously³³. Cisplatin assisted as positive control and was likewise formulated. The DMSO solution considered as negative control.

Colony formation. To determine the capability of proliferative activity and long-lasting survival aptitude of cancer cells colony formation assay was performed in a 6-well plate. The colony forming assay was performed as those stated previously³³. Different concentration of citral was used to determine the colony formation of cell lines. Cell colony was stained by crystal violet, counted and graphically plotted. All statistical analysis were performed.

Wound healing Assay. The assay was performed according to the previous method³³. The citral was used as dose-dependent manner and the cells were stained by crystal violet.

Light microscopy. The density of 2 × 10⁴ cells per well were seeded on to 96-well culture plates and allowed to grow for 24 h. Then different concentration of citral were treated as previously described³³. The morphological changes of cell images of both treated and untreated cells was captured a Leica DMIL LED equipped with an Integrated 5.0 Mega-Pixel MC 170 HD camera (Wetzlar, Germany).

Go terms	Go ids	Category	p-value	Genes
BP	GO:0006915	Apoptotic process	0.45	EDAR
BP	GO:0043154	Negative regulation of cysteine-type endopeptidase activity involved in apoptotic process	0.95	IFI6
BP	GO:0043065	Positive regulation of apoptotic process	0.33	IFIT2
BP	GO:0043066	Negative regulation of apoptotic process	0.50	DHRS2
BP	GO:1990086	Lens fiber cell apoptotic process	0.04	E2F2
BP	GO:0043066	Negative regulation of apoptotic process	0.50	IFIT3
BP	GO:0043066	Negative regulation of apoptotic process	0.50	CEACAM5
BP	GO:0043524	Negative regulation of neuron apoptotic process	0.09	XRCC2
BP	GO:0043066	Negative regulation of apoptotic process	0.50	PLK1
BP	GO:0043065	Positive regulation of apoptotic process	0.33	TOP2A
BP	GO:0006915	Apoptotic process	0.45	CDK1
BP	GO:0043066	Negative regulation of apoptotic process	0.50	CDK1
BP	GO:0006919	Activation of cysteine-type endopeptidase activity involved in apoptotic process	0.88	IFI27
BP	GO:0006915	Apoptotic process	0.45	ESPL1
BP	GO:0043154	Negative regulation of cysteine-type endopeptidase activity involved in apoptotic process	0.95	LAMP3
BP	GO:0043066	Negative regulation of apoptotic process	0.50	ASNS
BP	GO:0006915	Apoptotic process	0.45	BUB1B
BP	GO:0006915	Apoptotic process	0.45	PLSCR1
BP	GO:0042981	Regulation of apoptotic process	0.67	INHBE
BP	GO:0006915	Apoptotic process	0.45	TPX2
BP	GO:0006919	Activation of cysteine-type endopeptidase activity involved in apoptotic process	0.88	TNFSF15
BP	GO:0006915	Apoptotic process	0.45	BUB1
BP	GO:0043065	Positive regulation of apoptotic process	0.33	APBB2
BP	GO:0043066	Negative regulation of apoptotic process	0.50	APBB2
BP	GO:0006915	Apoptotic process	0.45	MCM2
BP	GO:0006915	Apoptotic process	0.45	NTN1
BP	GO:0006915	Apoptotic process	0.45	TNS4
BP	GO:0002903	Negative regulation of B cell apoptotic process	0.53	AURKB
BP	GO:0043066	Negative regulation of apoptotic process	0.50	MAD2L1
BP	GO:0043065	Positive regulation of apoptotic process	0.33	PLEKHG2
BP	GO:0006915	Apoptotic process	0.45	TRAF5
BP	GO:0042981	Regulation of apoptotic process	0.67	TRAF5
BP	GO:0043065	Positive regulation of apoptotic process	0.33	MELK
BP	GO:0006915	Apoptotic process	0.45	MELK
BP	GO:0006915	Apoptotic process	0.45	CHI3L1
BP	GO:0043065	Positive regulation of apoptotic process	0.33	SRC
BP	GO:0043066	Negative regulation of apoptotic process	0.50	SRC
BP	GO:0043154	Negative regulation of cysteine-type endopeptidase activity involved in apoptotic process	0.95	SRC
BP	GO:0042981	Regulation of apoptotic process	0.67	TNFRSF1B
BP	GO:0006915	Apoptotic process	0.45	KANK2
BP	GO:0043066	Negative regulation of apoptotic process	0.50	BTC
BP	GO:0043065	Positive regulation of apoptotic process	0.33	BARD1
BP	GO:0043066	Negative regulation of apoptotic process	0.50	BARD1
BP	GO:2000352	Negative regulation of endothelial cell apoptotic process	0.10	SERPINE1
BP	GO:0043524	Negative regulation of neuron apoptotic process	0.09	TERT
BP	GO:2000352	Negative regulation of endothelial cell apoptotic process	0.10	TERT
BP	GO:0043065	Positive regulation of apoptotic process	0.33	NUPR1
BP	GO:0043065	Positive regulation of apoptotic process	0.33	NTSR1
BP	GO:0043066	Negative regulation of apoptotic process	0.50	NTSR1
BP	GO:0043065	Positive regulation of apoptotic process	0.33	RPS6KA2
BP	GO:0043065	Positive regulation of apoptotic process	0.33	TGM2
BP	GO:0043066	Negative regulation of apoptotic process	0.50	TGM2

Table 5. The identified down-regulated genes list after citral treatment in AGS cell lines. BP: Biological process.

RNA isolation. AGS cell lines were cultured in 25 cm² cell culture flasks and treated with different concentration of citral. After 48 h, the total RNA content was extracted by using RNeasy mini kit (Qiagen, Hilden, Germany). The isolated RNA was used for RNA sequencing.

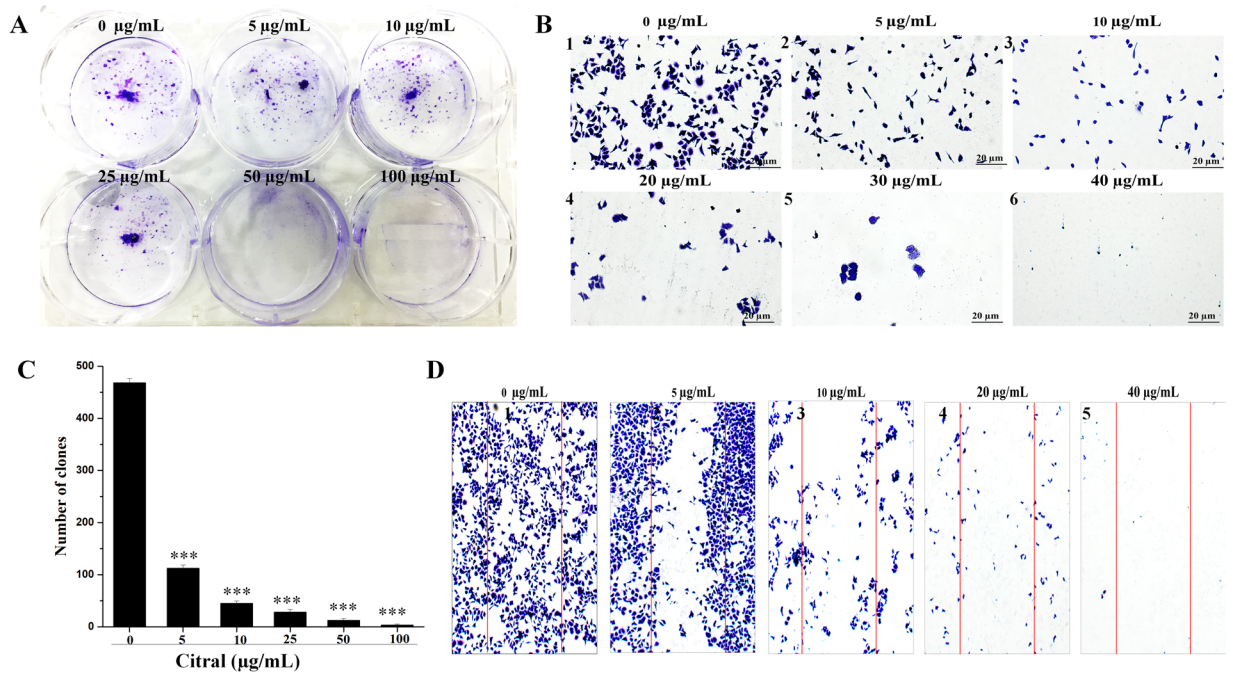


Figure 8. The colony progress and invasive ability of AGS citral treatment (with or without) (A,B). Cells were seeded uniformly (1×10^5) and grown for 4 days. The crystal violet staining were used to detect the colonies. Based on dose-dependent (citral) the cells clearly exhibited growth inhibition. (C) The total number of colonies in with or without treatment were measured using imageJ software and plotted graphically (Fig. 2C). (D) The effect of citral has reduced down the migration cells associated to that of untreated cells and migration ability decreased with increasing concentration of citral treatment (Fig. 2D2–D5). The images are representative of three independent replicates. Each bar represents the mean \pm SE of duplicate samples of three independent experiments (** $P < 0.001$ using student's t-test).

RNA sequencing and read mapping. In this study, the paired end (PE) RNAseq libraries of control and citral treated samples were prepared by using Truseq Stranded mRNA Prep Kit (Illumina) according to manufacture protocol. Then constructed RNAseq libraries were sequenced by Illumina Hiseq 2500 platform to obtain 101 base pair length reads. The generated each raw reads quality, removal of adaptor sequences, and low quality reads filtration was accessed through FASTX-Toolkit (http://hannonlab.cshl.edu/fastx_toolkit/). Further, obtained high quality reads were aligned with human genome (hg19) sequences using Tophat v2.0.13³⁴ with default parameters and transcript expression was estimated with cuffdiff v.2.2.0³⁵ using h19 genome annotations. The relative abundance of transcripts was normalized and measured in fragments per kb of exon per million fragments mapped (FPKM)³⁶.

Differential expressed genes and functional enrichment analysis. Cuffdiff from Cufflinks repository was used to identify differential expressed genes (DEGs) by comparing gene expression levels from control and citral treated groups. Further, Cuffdiff processed data was used to generate expression plots (Supplementary Fig. 2) using CummeRbund (<http://compbio.mit.edu/cummeRbund/>). The significant DEGs were selected with threshold of fold change more than 2 and P-value less than 0.05 by comparing control and citral treated groups. Initially, the up-regulated genes are selected for the functional enrichment analysis using the FunRich 3.1.3 tool. Where the distance between the nodes is set as 150 for producing the up-regulated gene network and up-regulated genes interacting with other relative genes (external genes).

Further, the gene list is considered to identify the significant Gene Ontology (GO) and to visualize the GO interaction network utilizing BiNGO 3.0.3 application in Cytoscape 3.6.1^{37–39}. Further, functional enrichment analysis including GO and Kyoto Encyclopedia of Genes and Genomes (KEGG) pathway analysis was performed to the selected DEGs (fold change ≥ 2) using DAVID Bioinformatics Resources 6.8 to identify the apoptotic relative genes⁴⁰. (<https://david.ncifcrf.gov>).

Apoptotic cell propidium iodide staining. The propidium iodide staining assay was performed according to the previous method³³. The appropriate number of AGS cell lines were seeded (5×10^4 /well) and treated with citral (10 and 20 µg/mL). The cells undergone apoptotic process were detected under fluorescence microscope using a Leica DMLB fluorescence microscope (Wetzlar, Germany).

Hoechst staining. AGS cell lines (2×10^5 /well) were seeded and analyzing the apoptotic effect by citral in different concentration was measured by Hoechst staining 33342. The assay was performed according to the

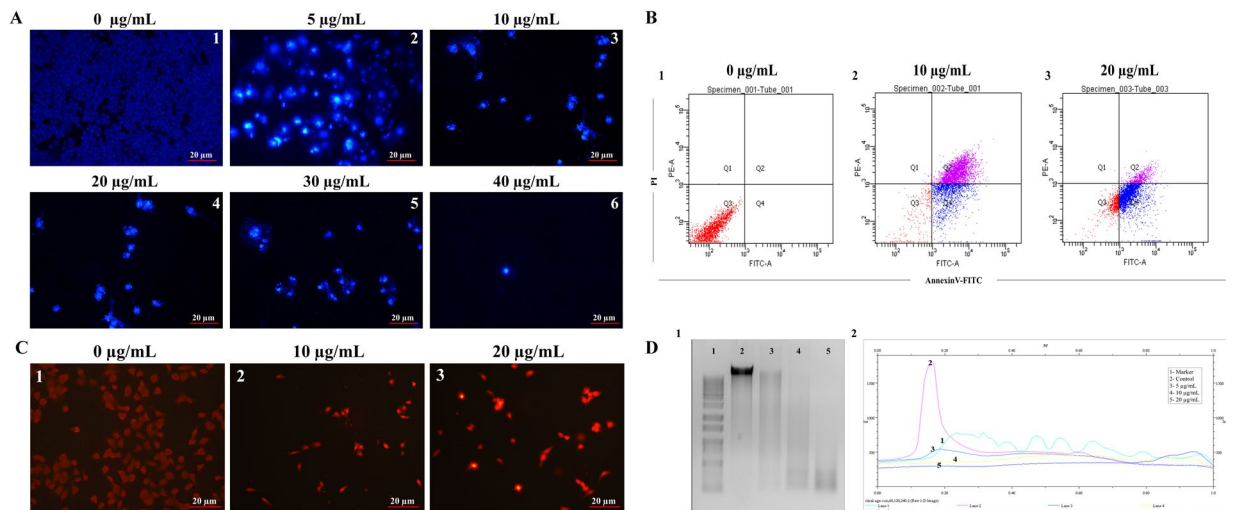


Figure 9. Citral induced apoptosis in AGS cell lines. **(A)** DNA condensation and nuclear staining of AGS cells with or without citral treatment. **(B)** Flow cytometry analysis of cancer cells with or without treatment. Expressive figures displaying the population of live cells (annexin V–PI–), early apoptotic (annexin V+PI–), late apoptotic cells (annexin V+PI+) and necrotic cells (annexin V–PI+). **(C)** PI staining of AGS cells with or without citral treatment. The cells remained intact don't allow cells to stain with the dye. However, the damage cells were stained with PI and indicated the apoptotic cells. **(D)** DNA fragmentation analysis was carried out after isolation of genomic DNA from AGS with or without different concentration of citral treatment. 1. DNA ladder 1 kb; 2. Control; 3. 5 µg/mL; 4. 10 µg/mL; 5. 20 µg/mL.

previous method³³. The images were captured under fluorescence microscope using a Leica DMLB fluorescence microscope (Wetzlar, Germany).

DNA fragmentation assay. The proper amount of cells were seeded and allowed for overnight to become well differentiated. The assay was performed according to the previous method³³. After cell adhesion, citral was used at different concentration (5, 10 and 20 µg/mL) for the treatment. The gel was then examined under ultraviolet light and photographed.

Data Availability

All the sequences were submitted to NCBI-SRA under accession number SRP150561.

References

1. Ferro, A. *et al.* Worldwide trends in gastric cancer mortality (1980–2011), with predictions to 2015, and incidence by subtype. *Eur. J. Cancer* **50**, 1330–44 (2014).
2. Jemal, A. *et al.* Global cancer statistics. *CA Cancer J. Clin* **61**, 69–90 (2011).
3. Cervantes, A. *et al.* Current questions for the treatment of advanced gastric cancer. *Cancer Treat. Rev* **39**, 60–67 (2013).
4. Montenegro, R. *et al.* BET inhibition as a new strategy for the treatment of gastric cancer. *Oncotarget* **7**, 43997–44012 (2016).
5. Panani, A. D. Cytogenetic and molecular aspects of gastric cancer: clinical implications. *Can lett.* **266**, 99–115 (2008).
6. Shu, S. *et al.* Response and resistance to BET bromodomain inhibitors in triple-negative breast cancer. *Nature*. **529**, 413–417 (2016).
7. Fong, C. Y. *et al.* BET inhibitor resistance emerges from leukemia stem cells. *Nature*. **525**, 538–542 (2015).
8. Priyadarsini, R. V. & Nagini, S. Cancer chemoprevention by dietary phytochemicals promises and pitfalls. *Curr. Pharm. Biotechnol* **13**, 125–136 (2012).
9. Arivazhagan, S., Kavitha, K. & Nagini, S. 1997. Erythrocyte lipid peroxidation and antioxidants in gastric cancer patients. *Cells Biochem. Funct* **15**, 15–18 (1997).
10. Guttenplan, J. B. Inhibition by L-ascorbate of bacterial mutagenesis induced by two N-nitroso compounds. *Nature* **268**, 368–370 (1997).
11. Khan, N., Afaq, F. & Mukhtar, H. Cancer chemoprevention through dietary antioxidants: progress and promise. *Antioxid. Redox. Signal* **10**, 475–510 (2008).
12. Carlini, E. A. *et al.* Pharmacology of lemongrass (*Cymbopogon citratus* Stapf). I. Effects of teas prepared from the leaves on laboratory animals. *J. Ethnopharmacology* **17**, 37–64 (1986).
13. Oh, T. Y. *et al.* Oxidative stress is more important than acid in the pathogenesis of reflux oesophagitis in rats. *Gut* **49**, 364–371 (2001).
14. Maruoka, T. *et al.* Lemongrass essential oil and citral inhibit Src/Stat3 activity and suppress the proliferation/survival of small-cell lung cancer cells, alone or in combination with chemotherapeutic agents. *Int. J. Oncol* **52**, pp 1738–1748 (2018).
15. Nigjeh, S. E. *et al.* Citral induced apoptosis in MDA-MB-231 spheroid cells. *BMC Complemen. Aletrnat. med* **18**, 56 (2018).
16. Ye, K. C. *et al.* Anticancer activity of the essential oil from *Cinnamomum longepaniculatum* leaves and its major component against human BEL-7402. *Acta. Anat. Sin* **43**, 381–386 (2012).
17. Elsayed, E. A., Sharaf-Eldin, M. & Wadaan, M. *In vitro* evaluation of cytotoxic activities of essential oil from *Moringa oleifera* seeds on Hela, HepG2, MCF-2, CaCo2 and L929 cells. *Asian. Pac. J. Cancer Prev* **16**(11), 4671–4675 (2015).
18. Crowley, C. & Waterhouse, N. Measuring survival of hematopoietic cancer cells with the colony forming assay in soft agar. *Cold Spring. Harb. Protoc* **8** (2016).
19. Wong, R. S. Apoptosis in cancer: from pathogenesis to treatment. *J. Exp. Clin. Cancer Res* **30**(1), 87 (2007).
20. Wang, J. *et al.* Cyclin dependent kinase 2 promotes tumor proliferation and induced radio resistance in glioblastoma. *Transl. Oncol* **9**(6), 548–556 (2016).

21. Chohan, T. A., Qian, H., Pan, Y. & Chen, J. Z. Cyclin dependent kinase 2 as a target for cancer therapy: progress in the development of CDK2 inhibitors as anti-cancer agents. *Curr. Med. Chem* **23**7–263 (2015).
22. Boer, L. D. *et al.* Cyclin A/cdk2 coordinates centrosomal and nuclear mitotic events. *Oncogene* **27**, 4261–4268 (2008).
23. Fiset, A. *et al.* 2011. Compartmentalized CDK2 is connected with SHP-1 and beta-catenin and regulates insulin internalization. *Cell Signal* **23**, 911–919 (2011).
24. Tian, A. *et al.* MDA-7/IL-24 induces Bcl-2 denitrosylation and ubiquitin-degradation involved in cancer cell apoptosis. *PLoS One* **7**(5), e37200 (2012).
25. He, H. & Sun, Y. Ribosomal protein S27L is a direct p53 target that regulates apoptosis. *Oncogene* **26**(19), 2707–16 (2007).
26. Nagata, S. Apoptosis and Clearance of apoptotic cells. *Annual review of immunology* **36**, 489–517 (2018).
27. Fernald, K. & Kurokawa, M. Evading apoptosis in cancer. *Trends Cell Biol* **23**(12), 620–633 (2009).
28. Asif, M. *et al.* Anticancer attributes of *Illiciumverum* essential oils against colon cancer. *S. Afr. J Bot* **103**, 156–161 (2016).
29. Kang, N. *et al.* Inhibition of EGFR signaling augments oridonin-induced apoptosis in human laryngeal cancer cells via enhancing oxidative stress coincident with activation of both the intrinsic and extrinsic apoptotic pathways. *Cancer Lett* **294**(2), 147–58 (2010).
30. Taylor, C., Cullen, P. & Martin, S. Apoptosis: controlled demolition at the cellular level. *Nature Reviews Molecular Cell Biology* **9**, 231–241 (2008).
31. Wyllie, A. H. Cell death: the significance of apoptosis. *Nature* **284**, 555–556 (1980).
32. Earnshaw, W. C. Nuclear changes in apoptosis. *CurrBiol* **7**, 337–343 (1972).
33. Perumalsamy, H. *et al.* Cellular effect of styrene substituted biscoumarin caused cellular apoptosis and cell cycle arrest in human breast cancer cells. *Int. J. Biochem. Cell. Biol* **92**, 104–114 (2017).
34. Trapnell, C., Pachter, L. & Salzberg, S. L. TopHat: discovering splice junctions with RNA-Seq. *Bioinformatics* **25**(9), 1105–11 (2009).
35. Trapnell, C. *et al.* Differential analysis of gene regulation at transcript resolution with RNA-seq. *Nat. Biotechnol* **31**(1), 46–53 (2013).
36. Mortazavi, A., Williams, B. A., McCue, K., Schaeffer, L. & Wold, B. Mapping and quantifying mammalian transcriptomes by RNA-seq. *Nat. Methods* **5**(7), 621–628 (2008).
37. Maere, S. & Heymans, M. Kuiper. BiNGO: a Cytoscape plugin to assess overrepresentation of Gene Ontology categories in biological networks. *Bioinformatics* **21**, 3448–3449 (2005).
38. Saito, R. *et al.* A travel guide to Cytoscape plugins. *Nat. Methods* **9**(11), 1069–76 (2012).
39. Pathan, M., Keerthikumar, S., Ang, C. S., Gangoda, L. & Quek, C. M. J. FunRich: a standalone tool for functional enrichment analysis. *Proteomics* **15**, 2597–2601 (2015).
40. Huangda, W., Sherman, B. T. & Lempicki, R. A. Systemic and integrative analysis of large gene lists using DAVID bioinformatics resources. *Nat Protoc* **4**(1), 44–57 (2009).

Acknowledgements

This work was supported by National Research Foundation grant (Grant No. 2017R1C1B5076111) and also supported by Cooperative Research Program for Agriculture Science and Technology Development (Project No. PJ0128132017), Republic of Korea.

Author Contributions

S.R.B. and H.P. designed the research, wrote the manuscript, performed the experiments and interpreted the results. S.N., and S.R. performed bioinformatics analysis. S.R.B. and Y.J.K conceived the project.

Additional Information

Supplementary information accompanies this paper at <https://doi.org/10.1038/s41598-019-41406-8>.

Competing Interests: The authors declare no competing interests.

Publisher's note: Springer Nature remains neutral with regard to jurisdictional claims in published maps and institutional affiliations.



Open Access This article is licensed under a Creative Commons Attribution 4.0 International License, which permits use, sharing, adaptation, distribution and reproduction in any medium or format, as long as you give appropriate credit to the original author(s) and the source, provide a link to the Creative Commons license, and indicate if changes were made. The images or other third party material in this article are included in the article's Creative Commons license, unless indicated otherwise in a credit line to the material. If material is not included in the article's Creative Commons license and your intended use is not permitted by statutory regulation or exceeds the permitted use, you will need to obtain permission directly from the copyright holder. To view a copy of this license, visit <http://creativecommons.org/licenses/by/4.0/>.

© The Author(s) 2019